

See discussions, stats, and author profiles for this publication at: <https://www.researchgate.net/publication/6935061>

Anodic Activation of PtRu/C Catalysts for Methanol Oxidation

ARTICLE in THE JOURNAL OF PHYSICAL CHEMISTRY B · MARCH 2005

Impact Factor: 3.3 · DOI: 10.1021/jp0461652 · Source: PubMed

CITATIONS

92

READS

23

4 AUTHORS, INCLUDING:



Qingye Lu

University of Alberta

21 PUBLICATIONS 434 CITATIONS

SEE PROFILE



Lin Zhuang

Wuhan University

90 PUBLICATIONS 3,186 CITATIONS

SEE PROFILE



Juntao Lu

Wuhan University

92 PUBLICATIONS 2,478 CITATIONS

SEE PROFILE

Anodic Activation of PtRu/C Catalysts for Methanol Oxidation

Qingye Lu, Bo Yang, Lin Zhuang,* and Juntao Lu

Department of Chemistry, Wuhan University, Wuhan 430072, China

Received: August 25, 2004; In Final Form: November 12, 2004

Anodic treatment of PtRu/C catalysts in 0.5 M sulfuric acid at 1.3 V (vs RHE) for 0.5 h was found able to promote the activity for methanol oxidation by a few tenths to 5 times. This anodic activation effect was valid for samples domestically prepared under different conditions and that produced by Johnson-Matthey. On the basis of the changes of cyclic voltammetry during the anodic treatment, a model was proposed for the activation effect. According to the model, there are two categories of ruthenium oxides in the catalyst: one is electrochemically reversible and beneficial for catalytic activity, while the other is irreversible and harmful. During the anodic treatment, the harmful oxide is decreased, while the beneficial oxide either increased or changed only slightly, resulting in a beneficial net change.

1. Introduction

Direct methanol fuel cells (DMFC) are regarded as promising new power sources in the future, especially for mobile and portable applications. In the development of DMFC, the catalysis for the methanol oxidation has been a major challenge. Since the advent of PtRu catalysts, the performance of DMFC has made a big step forward.^{1,2} Although numerous works have been reported concerning the different aspects of the PtRu catalyst, this system remains not fully understood because of its complexity. Accordingly, there may still be space for further improvement of the catalyst, and we shall show in this paper that a simple anodic treatment can lead to an appreciable improvement. This finding provides not only an effective technique to promote the performance but clues to the structure–activity relationship of the catalyst.

It is generally agreed that active-oxygen-containing surface species are necessary for the oxidative removal of CO-like poisoning intermediates on Pt surfaces.^{3–5} The promotion function of Ru in PtRu catalysts was attributed to the fact that Ru is more active than Pt in terms of promoting water discharge so that the onset potential of the formation of oxygen-containing surface species for Ru is lower than that for Pt.^{3,6–10} The optimum composition of PtRu has been a well-studied problem; many works have been devoted to this topic. The answer seems not so straightforward; the optimum percent of Ru in the alloy is a function of working temperature, methanol concentration, and electrode potential.^{4–5,11–18} The situation with nano PtRu catalysts is more complicated than that for the conventionally sized alloys. The Pt/Ru ratio in the nano alloy particles is difficult to control in preparation, and its X-ray diffraction (XRD) determination was even questioned by some authors.^{19–21} Moreover, in addition to alloy or metal particles, there is an appreciable amount of different forms of ruthenium oxides.^{20,22–31} These complexities in microscopic composition and structure lead to complicated structure–activity relationships, which are not yet well-understood for nanosized PtRu catalysts.

In recent years, Rolison and co-workers emphasized the importance of hydrous ruthenium oxides, which are highly

conductive, both electronically and protonically.^{19–20,32–33} In highlighting the function of hydrous oxides, they even denied the necessity of the alloy. But, direct evidence of the promotion function of hydrous oxides has been very limited. Los Alamos National Laboratory (LANL)³⁶ constructed a high-performance DMFC using an anode catalyst rich in hydrous ruthenium oxide. Arico^{34–35} and Lasch³⁸ prepared PtRu catalysts using preformed ruthenium oxides as the supports, but the best performance they obtained was no better than conventionally made PtRu catalysts. Very recently, Spinacé et al.³⁷ prepared a catalyst by spontaneous deposition of Pt on carbon-supported Ru nanoparticles and showed good performance for methanol electrooxidation, comparable to that of a commercial PtRu catalyst. They concluded that the formation of a PtRu alloy was not a required condition for effective methanol oxidation. It seems that the controversy concerning the governing factors of the nano PtRu catalysts is strongly related to the ruthenium oxide issue to which appropriate importance was not attached in early works.

In this paper, we show that the catalytic activity of nano PtRu/C can be remarkably promoted by anodic treatment, and this promotion effect is attributable mainly to favorable changes in the Ru oxides. It is demonstrated that there are two categories of Ru oxides: one is active, and the other is not only inactive but harmful. The two categories of oxides in a prepared catalyst can be manipulated electrochemically to improve the catalytic activity, and the changes can be characterized by cyclic voltammetry (CV).

2. Experimental Section

2.1. Electrochemical Experiments. All carbon-supported PtRu samples were prepared from H₂PtCl₆ and RuCl₃ using the improved impregnation method,³⁹ except for a commercial sample from Johnson-Matthey for comparison. The solvent for the precursor was ethanol or other, as stated. The Pt/Ru atomic ratio in the precursor was either 1:1 or 2:1; the supports included Vulcan XC-72 (Carbot), Printex XE-2 (Degussa), and a mixture of XC-72 and acetylene black (AB). A part of the catalyst comprising 20 wt % Pt + 10 wt % Ru/(XC72 + AB) was further treated in different ways to alter its composition, resulting in a number of new samples for study. A brief description was given in Table 1 for all samples tested.

* Corresponding author. E-mail: lzhuang@public.wh.hb.cn. Fax: +86-27-87647617.

TABLE 1: Collected Data Showing Universality of Anodic Activation

sample	ϕ (nm)	a (Å)	x_{Ru}	original mA/mg Pt		after activation mA/mg Pt (gain %)	
				0.4 V	0.5 V	0.4 V	0.5 V
A PtRu(20:10 wt %)/(XC72 + AB)	4	3.903	0.10	32	185	53 (65)	352 (93)
B sample A after 500 °C 2 h in H ₂ , shelved for 6 months	4.3	3.860	0.45	14	86	53 (278)	324 (277)
C sample A after 500 °C 2 h in Ar	3.6	3.878	0.30	5	41	32 (540)	232 (466)
D sample B after 120 °C in air				7	48	30 (329)	204 (325)
E sample B after 120 °C in air humidified with 60 °C water	3.8	3.857	0.47	9	65	45 (400)	312 (380)
F PtRu(20:5 wt %)/XC72, water as precursor solvent				37	270	66 (78)	515 (91)
G PtRu(20:10 wt %)/XC72, water as precursor solvent	2.8	3.881	0.27	62	360	90 (45)	572(59)
H PtRu(20:10 wt %)/XC72, Johnson–Matthey product	2.1	3.868	0.38	61	329	85 (39)	538 (64)
I PtRu (40:10 wt %)/XE2				34	230	64 (88)	370 (61)
J PtRu (40:20 wt %)/XE2, 120 °C 2 h in H ₂	2.6	3.893	0.18	36	215	54 (50)	382 (78)
K Pt Ru (40:20 wt %)/XE2, 120 °C 1 h in H ₂ and 1 h in Ar				37	215	73 (97)	430 (100)
L same as B, without shelving				12	82	74 (517)	440 (437)
M same as G, ethanol as precursor solvent	2.7	3.911	0.03	22	133	45 (105)	290 (118)
N PtRu(20:10 wt %)/XC72, 50 °C preheated	2.3	3.877	0.31	70	340	86 (23)	470 (38)
R PtRu(20:10 wt %)/XC72, 150 °C preheated	1.9	3.888	0.22	75	320	95 (27)	440 (38)
P PtRu(20:10 wt %)/XC72, 200 °C preheated	1.7	3.891	0.20	53	250	67 (26)	360 (44)
Q PtRu(20:10 wt %)/XC72, 250 °C preheated	2.9	3.906	0.08	51	245	66 (29)	360 (47)

The catalysts were deposited on a glassy carbon (GC) electrode ($\phi = 5$ mm) using the Nafion ink method.³⁹ Catalyst powder (10 mg) was dispersed ultrasonically in 1 mL diluted Nafion alcohol solution (0.05 wt %) to form an ink, and 5 μL of the ink was pipetted onto a GC disk electrode, which had been buff-polished with alumina suspension ($\phi = 0.05 \mu\text{m}$) prior to use. Although some investigators considered that the ink method was poorly reproducible,⁴⁰ our experiments proved that the error can be controlled to within ± 5 % by carefully controlling the details of experiment. One key point is to make sure that the catalyst was homogeneously dispersed in the ink with no visible grains or agglomerates attached on the wall of the glass container. It was also important to prevent methanol concentration changes due to prolonged measurement at elevated temperatures. The hydrogen bubbles produced from the counter electrode should be kept far from the working electrode.

The electrochemical experiments were conducted on a CHI-600A electrochemical system with a thermostatic electrochemical cell, and the reference electrode was a reversible hydrogen electrode (RHE).⁴¹ All solutions were prepared with deionized water (18 $\text{M}\Omega\cdot\text{cm}$).

2.2. X-ray Diffraction Analysis for Alloy Particle Size and Ru Percent. The XRD pattern for the catalyst was obtained on a Shimadzu XRD-6000 X-ray diffractometer using a Cu K α radiation source operating at 40 kV and 30 mA. The characteristic reflections of Pt face-centered cubic (fcc) structure were clearly shown by XRD, while no visible peaks related to tetragonal RuO₂ or hexagonal close-packed (hcp) Ru phases were found (Figure 1).

The Pt(220) peak was fitted to a Gaussian line shape on a linear background using the Levenberg–Marquardt algorithm so that the position of the peak maximum (θ_{max}) and the full-width at half-maximum ($B_{2\theta}$) can be obtained precisely.

The lattice parameter of the Pt fcc crystal, a , was calculated from θ_{max} according to Vegard's law:

$$a = \frac{\sqrt{2}\lambda_{\text{K}\alpha 1}}{\sin \theta_{\text{max}}} \quad (1)$$

where $\lambda_{\text{K}\alpha 1} = 0.154\,056$ nm.

The diameter of PtRu nano particles, ϕ , was calculated according to the Scherrer formula:

$$\phi = \frac{0.9\lambda_{\text{K}\alpha 1}}{B_{2\theta} \cos \theta_{\text{max}}} \quad (2)$$

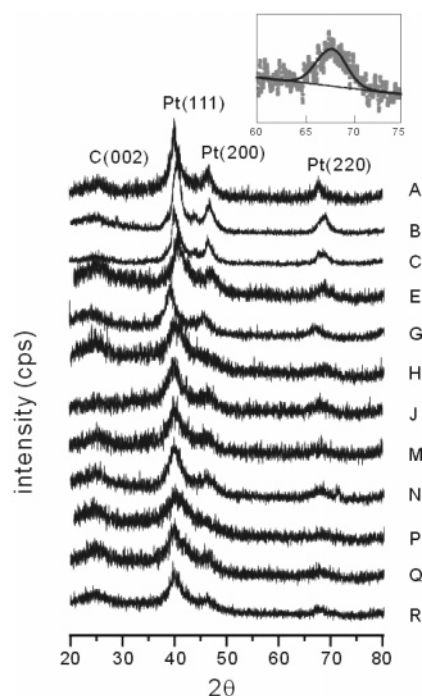
The thus-calculated sizes were in good agreement with those obtained by high-resolution transmission electron microscopy (HRTEM) in our experiments.³⁹

The Ru atomic fraction in the alloy, x_{Ru} , was calculated from XRD data using the formula proposed by Antolini et al.:^{42–43}

$$a = a_0 - 0.124x_{\text{Ru}} \quad (3)$$

where a_0 is the lattice constant of pure Pt. In the case of unsupported pure Pt, $a_0 = 0.392\,31$; while for supported pure Pt, $a_0 = 0.39155$, which was obtained from XRD measurement of the Pt/C made by E-TEK.⁴³

Equation 3 is similar to the formula reported by Radmilović et al.⁴⁴ for single-phase Pt–Ru bulk alloys: $a = 3.9262 - 0.1249x_{\text{Ru}}$ (or $a = 3.8013 + 0.1249x_{\text{Pt}}$). The validity of eq 3 was checked by the reasonable agreement between the x_{Ru} values deduced using this equation and the values from X-ray fluorescence for the arc-melting Pt–Ru alloys reported by Gasteiger et al.¹⁵ The a , ϕ , and x_{Ru} values deduced from XRD data are listed in Table 1.

**Figure 1.** XRD patterns of samples tested in this work.

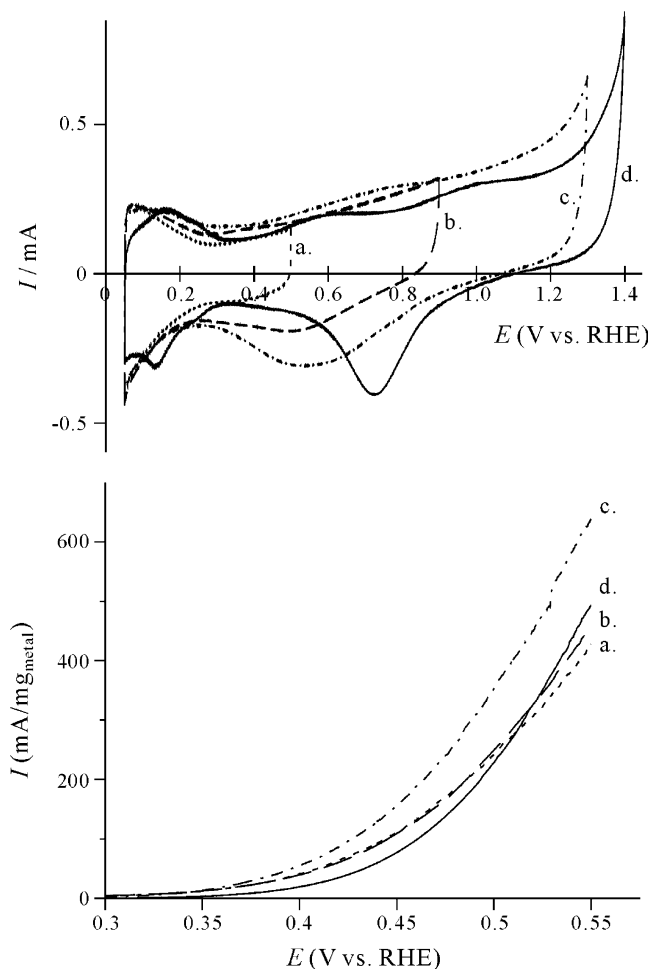


Figure 2. CV and methanol oxidation curves of sample G after potential scans to different positive extremes. Potential scans performed in 0.5 M H_2SO_4 ; MeOH oxidation in the same solution (60 °C) with 1 M MeOH added. Curves a, b, c, and d correspond to situations after 20 cycles of CV scans with positive extremes 0.5, 0.9, 1.3, and 1.4 V (RHE), respectively. Scan rate was 20 mV/s for CV and 1 mV/s methanol oxidation.

2.3. Thermal Analysis. Thermogravimetric analysis (TGA) and differential thermal analysis (DTA) were simultaneously carried out on a NETZSCH STA 449C. Samples were tested over the temperature range from room temperature to 800 °C at 10 °C/min under flowing, ultrapure N_2 . Weight loss was observed in the range ~150–550 °C and attributed to the structural water of hydrous ruthenium oxides, RuO_xH_y .²⁰ The thermal analyses indicated that there was a greater or lesser quantity of hydrous ruthenium oxides in all samples tested. The oxides mentioned in the following text may be different forms of hydrous oxides, but we shall call them different oxides for simplicity.

3. Results and Discussion

3.1. Anodic Activation of PtRu/C for Methanol Oxidation.

In published works, CV characterization of PtRu catalysts was usually performed at potentials no more than 1.0 V (vs RHE) to prevent the loss of ruthenium.^{45,46} However, we found that anodic treatment at appropriately higher potentials could remarkably improve the catalytic activity of PtRu/C for methanol oxidation. Figure 2 shows the promotional effects of CV scans. The CV scans were performed with different positive extreme potentials for 20 cycles, and the CV curves in Figure 2 were the last cycles for each set of scans. As shown in the figure,

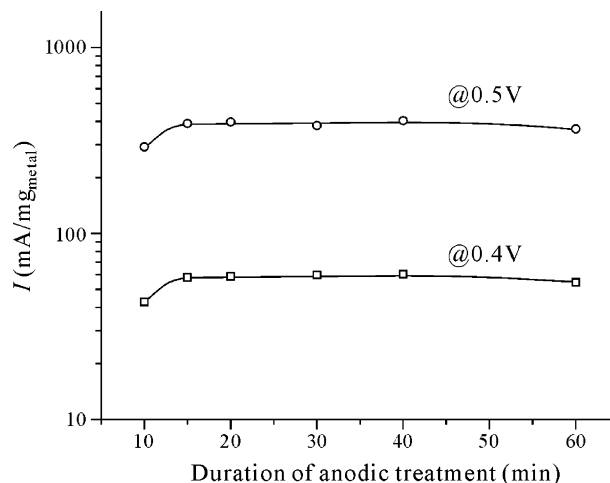


Figure 3. Methanol oxidation activity at 0.4 and 0.5 V (of sample G) as functions of the duration of anodic treatment at 1.3 V in 0.5 M H_2SO_4 at 60 °C.

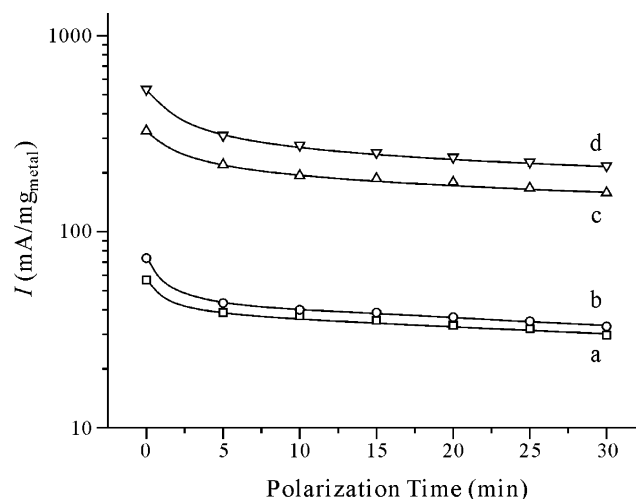


Figure 4. Durability of the catalytic activity gained in anodic treatment (of sample G) in 1 M MeOH + 0.5 M H_2SO_4 at 60 °C. Curves a and b are methanol oxidation currents at 0.4 V before and after anodic treatment, respectively; c and d are analogous curves for 0.5 V.

when the positive extreme potential was below 1.0 V, there was little effect on the MeOH oxidation. When the positive extreme increased to 1.3 V, 20 cycles of CV scans brought about appreciable improvement in the catalytic activity. In the working potential region prevailing in direct methanol fuel cells (~0.4–0.45 V vs RHE), a gain in activity of about 50% was obtained for the sample shown. However, if the positive extreme was further increased to 1.4 V, the activity would be decreased. In that case, the CV of the catalyst was found to have become similar to that of pure Pt, indicating excessive loss of Ru.

The anodic activation can be performed more easily by steady-state polarization at 1.3 V instead of potential scans. Figure 3 shows an example of the dependence of the activation effect on the duration of anodic treatment at 1.3 V. The activity increases first and levels off, followed by a slight decrease for prolonged treatment. The optimized duration was about 15–45 min, not very critical. In the later works, 1.3 V for 30 min was taken as routine. The gained activity was found essentially as stable as the original activity (Figure 4).

Table 1 shows the results for all samples tested. These samples included variations in carbons support, solvent used in catalyst preparation, preheat treatment before reduction in hydrogen flow (samples N, R, P, and Q), atmosphere, and

temperature of posttreatment. A commercial catalyst (sample H, from Johnson-Matthey) was also tested for comparison. All samples showed the activation effect with an activity gain ranging from a few tenths to about 5 times. It proves that the anodic activation effect is quite universal. A larger activation effect was found for samples with lower original activities. The anodic activation was also tested with an assembled DMFC. After the anodic treatment on the anode made from PtRu/C catalyst, the activity of the anode toward methanol oxidation was indeed improved appreciably.

3.2. CV Changes Caused by Anodic Treatment. To get an insight into the anodic activation, the process of anodic treatment was followed by CV characterization. Though CV has been widely used for the characterization of PtRu catalysts, there was a lack of systematic reporting on the CV features. We carefully investigated the CV curves of a number of typical PtRu/C catalysts and found that a combination of narrow (~ 0.05 – 0.40 V) and wide (~ 0.05 – 1.30 V) CV measurements was much more informative than wide scans only. A detailed study on the CV feature in conjunction with XRD and thermal analysis will be reported elsewhere, and the main points are briefed as follows.

The general CV features of PtRu/C catalysts were found similar to those of metallic Ru. At the low-potential region, there are both cathodic current for hydrogen adsorption and anodic current for the oxidation of adsorbed hydrogen. The hydrogen adsorption–desorption is quite reversible. In the narrow CV, the cathodic and anodic branches are approximately mirror-symmetrical. The CV of PtRu/C in the hydrogen adsorption region shows featureless curves, quite different from those of Pt, which exhibit two or three characteristic peaks. In the wide CV scan, a relatively large anodic current appeared for potentials above 0.8 V, but the current peak was not well-developed in the potential range studied. On the reverse scan, a prominent cathodic current peak corresponding to the anodic current peak appeared at a rather low potential, indicating an irreversible nature of the process attributable to the redox reaction of some kind of ruthenium oxide. The cathodic current peak for the reduction of surface oxides of Pt expected to occur round 0.8 V usually does not appear for PtRu/C catalysts. The oxides seen on the CV for PtRu/C catalysts are not only those formed from the alloyed Ru during CV operation but also those originally existing in the catalyst as prepared. The ruthenium oxides in PtRu/C can be divided into two categories in terms of electrochemical reversibility: one reversible and the other irreversible. Different reports about the reversibility of ruthenium oxides can be found in the literature. High reversibility is desirable for supercapacitor applications, but not all ruthenium oxides are reversible.^{47–49} In the following, we shall show that the two categories of ruthenium oxides in PtRu/C behave differently in the anodic treatment and methanol oxidation. The CV change due to anodic treatment for the carbon support is shown in Figure 5. After the anodic treatment, the CV curve shape remained basically unchanged, but the capacitance was somewhat increased. The absolute value of CV current change of the carbon support was much smaller than those for PtRu/C samples (Figures 2, 6, and 7). Besides, in PtRu/C samples, an appreciable part of the carbon support surface was covered with the catalyst particles, and the effectively exposed electrochemical surface area of the carbon support in PtRu/C should be notably smaller than that in the pure carbon sample, but the actual value was unknown. For simplicity, in the following discussions, the change of support during anodic treatment will be neglected.

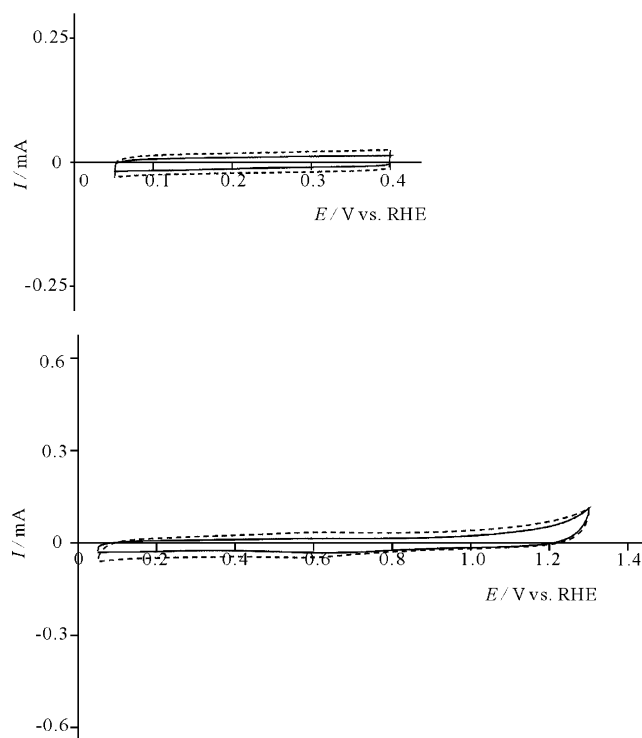


Figure 5. CVs of an electrode loaded with the same amount of carbon black as that for Figure 7 in 0.5 M H_2SO_4 at 60°C , 20 mV/s, before (solid line) and after (dashed line) anodic treatment. Current scale is set to the same as that in Figure 7 for convenient comparison.

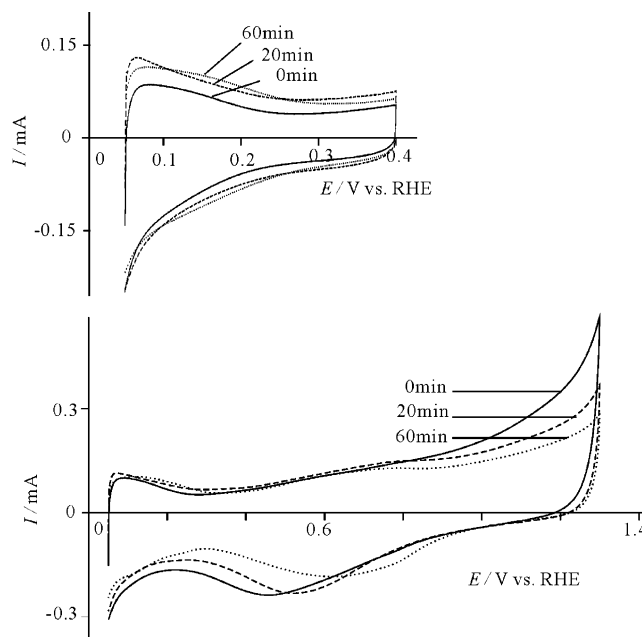


Figure 6. CV changes during anodic treatment of high alloy degree sample (sample B) in 0.5 M H_2SO_4 at 60°C , 20 mV/s.

The CV curves before and after anodic treatments are given in Figures 6 and 7 for two typical samples. Figure 6 is a sample representing the high-alloy-degree cases. The anodic treatment caused the curves of narrow potential range CV to shift upward and downward by about the same displacement for the anodic and cathodic branches, respectively. It indicates an addition of a potential independent capacity, which is characteristic of reversible hydrous ruthenium oxides. This oxide should be the result of oxidation of the alloyed Ru. In contrast, the CV of a wide potential range shows a continuous decrease in irreversible ruthenium oxides. This example reveals that the reversible and

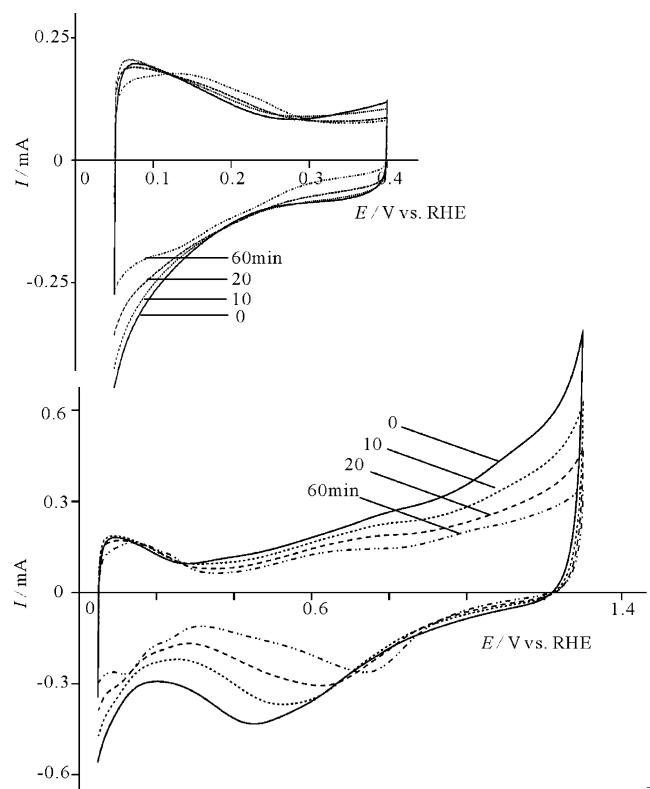


Figure 7. CV changes during anodic treatment of low alloy degree sample (sample G) in 0.5 M H₂SO₄ at 60 °C, 20 mV/s.

irreversible oxides are two different species, and the irreversible current peaks seen on wide CV are not the result of the further oxidation of the reversible oxide seen on narrow CV. If the reversible and irreversible oxides were due to the same species and only differed in oxidation state, the charge enveloped by the CV curve would have changed in parallel for the narrow and wide potential scans. Figure 7 exemplifies the low-alloy-degree catalysts. Like Figure 6, the charge of wide CV decreased continuously during anodic treatment, but the charge of narrow CV decreased, too, in contrast to Figure 6.

If it is assumed that the reversible oxide can not only be generated from the alloyed Ru but also be dissolved gradually during the anodic treatment, the apparent difference of the two examples can be interpreted with a unified model. The change in the narrow CV charge during the anodic treatment is mainly determined by the competition of the anodic generation and anodic dissolution of the reversible oxide. When the Ru alloy degree is high, the rate of reversible oxide generation exceeds the dissolution, resulting in a net increase of the reversible oxide. The opposite is true for catalysts with low Ru alloy degrees. Unlike the reversible oxide, the irreversible oxide always decreases in anodic treatment. Because the redox reaction of the irreversible oxide does not take place in the narrow potential scan range, the narrow CV is not affected by the change of irreversible oxide. In contrast, the wide CV is influenced by both the reversible and irreversible oxides.

3.3. Possible Reasons for the Anodic Activation. These discussions indicate three main changes caused by the anodic treatment to the catalysts: the decrease in Ru alloy degree, the decrease in irreversible Ru oxide, and the change in reversible oxide, with the latter depending on the original alloy degree of the catalyst. They are the major candidates for the causes of anodic activation effect for PtRu/C catalysts. The cleaning process of the catalyst surface during anodic treatment may also contribute to the anodic activation effect. However, it should

TABLE 2: Process of Anodic Treatment of Sample B (alloy degree $x_{\text{Ru}} = 0.45$)'

time sequence	anodic duration (min)	Q_n (mC)	Q_w (mC)	A_m at 0.4 V (mA/mg Pt)	A_m at 0.5 V (mA/mg Pt)
1	0	2.15	15.7	14	86
2	4	2.9	15.0	37	225
3	10	2.8	14.3	45	233
4	13	3.05	13.7	46	273
5	20	2.85	13.5	49	282
6	30	2.85	12.9	53	324
7	40	2.85	12.4	52	313

TABLE 3: Process of Anodic Treatment of Sample G ($x_{\text{Ru}} = 0.27$)'

time sequence	anodic duration (min)	Q_n (mC)	Q_w (mC)	A_m at 0.4 V (mA/mg Pt)	A_m at 0.5 V (mA/mg Pt)
1	0	4.8	26.7	62	360
2	10	4.75	21.6	71	462
3	15	4.6	19.3	88	586
4	20	4.5	17.8	88	598
5	30	4.35	16.7	90	572
6	40	4.2	15.8	91	608

not be the main cause of anodic activation, because it cannot account for the observed correlation between the CV curve change and activation discussed in the following section.

3.3.1. Influence of Change in Alloy Degree. The optimal alloy degree has been a topic of study for a long time, but the situation appears quite complicated. Because pure Ru is inactive for methanol oxidation and PtRu is always better than pure Pt, it is natural to assume a volcano-shaped relationship. However, quite different data were found in the literature. It seems that the optimal Ru % depends on the conditions of catalyst preparation, the form of the catalysts (bulk alloy or nano particles, with or without supports, etc.), and the definition of Ru % (in precursors or in products, in all valence states, or in zero valence only). Besides, the measurement conditions may also be an influence. For example, Gasteiger et al.^{14–15} studied arc-melting polycrystalline alloy and found 10% alloy degree to be the best for room temperature and 33% for 60 °C. For nano PtRu catalysts, the situation is even more complicated because of the multiple-composition nature. Rolison et al.^{19–20,32–33} stressed the function of Ru hydrous oxide and denied completely the necessity of alloy. In our case, it is noted that the anodic activation was effective regardless of the wide range of the original alloy degrees. For example, the sample with the highest alloy degree (sample E, $x = 0.47$) and the sample with the lowest alloy degree (sample M, $x = 0.03$) in Table 1 both show remarkable improvement after anodic treatment. There may be two possibilities behind this fact. One is that the alloy degree has little effect on the catalytic activity, or at least this effect is much weaker than other influencing factors. Another possibility is that the best alloy degree is well below 3%, in agreement with Rolison's claim. In view of the finding described in the next section (3.3.2), the loss of an excess of alloyed Ru can be excluded from being the main cause of the activation effect of anodic treatment, even if the optimal Ru % should be close to zero.

3.3.2. The Influence of Changes in Ru Oxides. To investigate the influence of the reversible and irreversible oxides, the changes of CV parameters and mass activity were systematically studied as functions of anodic treatment time for the two typical samples shown in Figures 6 and 7, and the relevant data are listed in Tables 2 and 3. A variety of chemoinformatics approaches were tried on the collected data, and finally, an

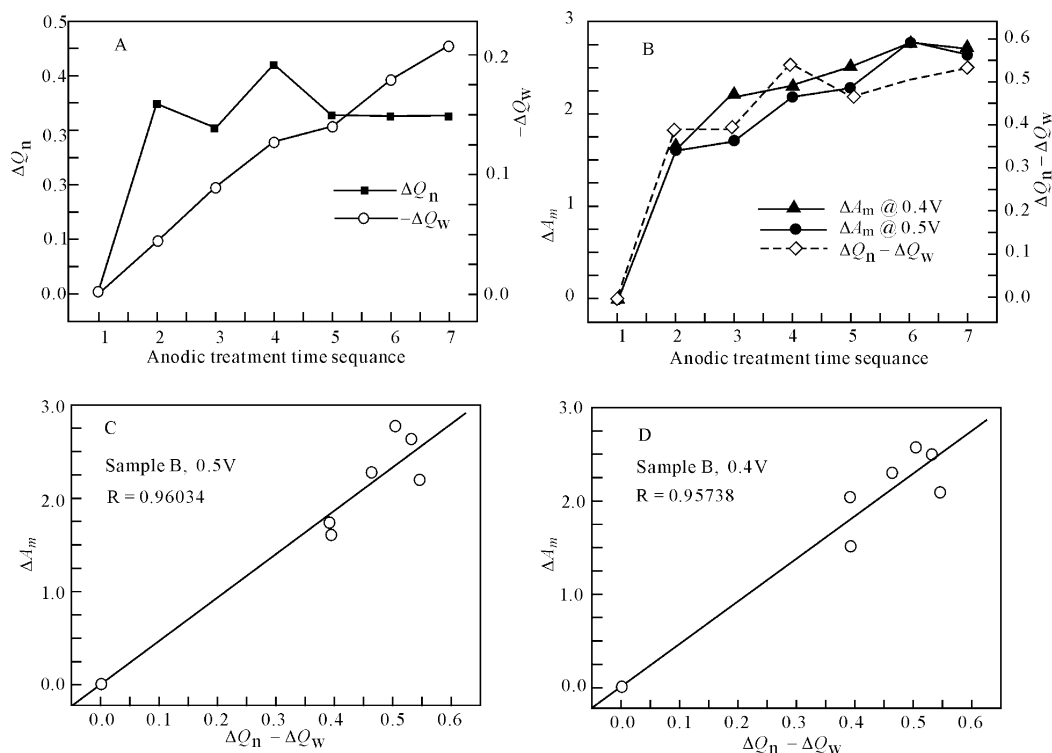


Figure 8. Linear fitting of eq 4 for sample B.

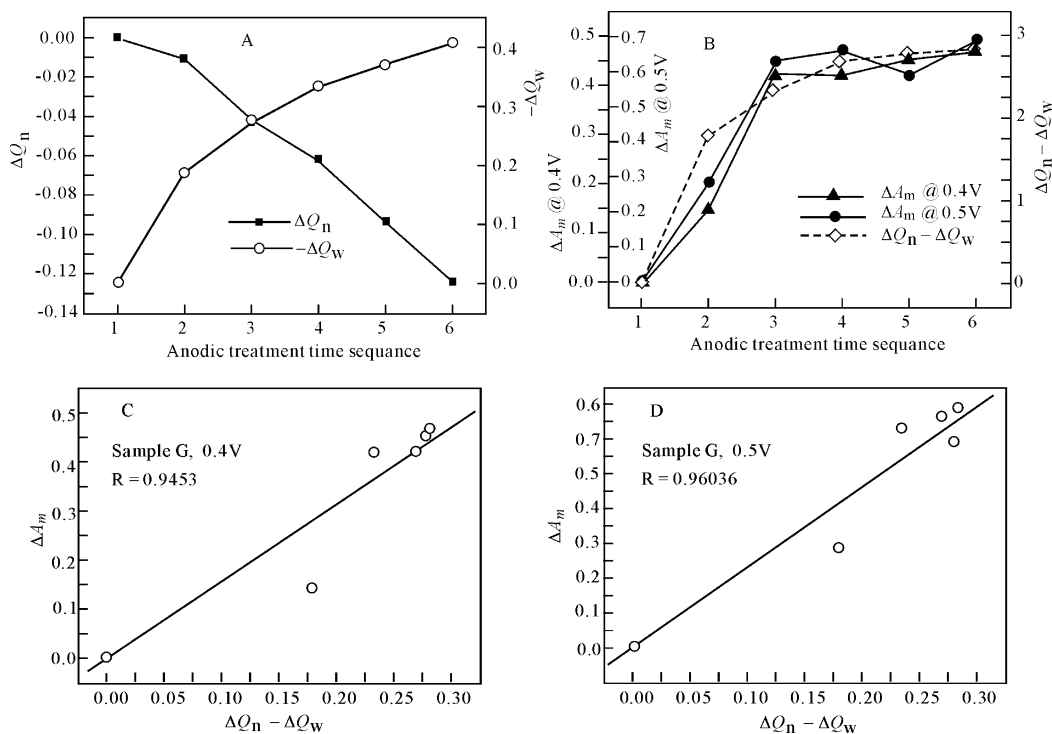


Figure 9. Linear fitting of eq 4 for sample G.

empirical linear relationship was found between the change of mass activity, A_m , and the change of CV charges, Q :

$$\Delta A_m = k(\Delta Q_n - \Delta Q_w) \quad (4)$$

In eq 4, $\Delta A_m = (A_m - A_{m,0})/A_{m,0} = \delta A_m/A_{m,0}$, $\Delta Q_n = (Q_n - Q_{n,0})/Q_{n,0} = \delta Q_n/Q_{n,0}$, and $\Delta Q_w = (Q_w - Q_{w,0})/Q_{w,0} = \delta Q_w/Q_{w,0}$, where subscript 0 indicates the situation before anodic treatment and n and w stand for narrow and wide CV scans,

respectively. The validity of eq 4 is illustrated by Figures 8 and 9.

Figure 8 is representative for high-Ru-alloy degree catalysts. Figure 8a shows that both ΔQ_n and $-\Delta Q_w$ increase during anodic treatment but in somewhat different ways. In Figure 8b, the values of ΔA_m for 0.4 and 0.5 V are plotted together with $(\Delta Q_n - \Delta Q_w)$ as functions of the time sequence of anodic treatment. The three curves appear in good coincidence. Figure 8c,d shows plots of ΔA_m versus $(\Delta Q_n - \Delta Q_w)$ for 0.4 and 0.5 V, respectively, and shows a satisfactory regression coefficient

for passing-through-origin fitting. Figure 9 differs from Figure 8 in that ΔQ_n decreases with time owing to low alloy degree. Despite that, the linear fitting in Figure 9 comes out to be as good as in Figure 8.

Because ΔQ_n and ΔQ_w reflect roughly the changes in the amount of reversible and irreversible Ru oxides, respectively, the validity of eq 4 strongly suggests that Ru oxides are very important and the two kinds of oxides play opposite roles in PtRu/C catalysts: the reversible oxide is beneficial, while the irreversible one is harmful. The anodic treatment promotes the catalyst by reducing the amount of irreversible Ru oxide and for high alloy samples also by increasing the amount of reversible Ru oxide.

It is worth noting that the slope k in Figure 8 is larger than that in Figure 9. This difference can be explained by the difference between the change of CV charge and the change of oxides, based on the assumption that the Ru oxide changes are the major cause of the anodic activation. If we assume that the normalized gain in activity is proportional to the normalized gain of reversible oxide minus the normalized gain of irreversible oxide, that is

$$\Delta A_m = k^*(\Delta Q_{re} - \Delta Q_{irr}) \quad (5)$$

the above-mentioned difference in k is understandable. In eq 5, the normalized gains in oxides are defined in a way similar to the normalized gain of CV charges: $\Delta Q_{re} = (Q_{re} - Q_{re,0})/Q_{re,0} = \delta Q_{re}/Q_{re,0}$ for the reversible oxide and $\Delta Q_{irr} = (Q_{irr} - Q_{irr,0})/Q_{irr,0} = \delta Q_{irr}/Q_{irr,0}$ for the irreversible oxide. Unfortunately, we were not able to extract $(\Delta Q_{re} - \Delta Q_{irr})$ from experimental data for the time being, so we had to plot according to eq 4 instead of eq 5. It can be easily realized that ΔQ_n and ΔQ_w are related to but differ from ΔQ_{re} and ΔQ_{irr}

$$\Delta Q_n = \delta Q_{re}/(Q_{re,0} + C_n) = \Delta Q_{re}Q_{re,0}/(Q_{re,0} + C_n) \quad (6)$$

$$\Delta Q_w = (\delta Q_{irr} + w \delta Q_{re})/(Q_{irr,0} + Q_{re,0} + C_w)$$

or

$$\Delta Q_w = \Delta Q_{irr}Q_{irr,0}/(Q_{irr,0} + Q_{re,0} + C_w) + w \delta Q_{re}/(Q_{irr,0} + Q_{re,0} + C_w) \quad (7)$$

where C_n and C_w are the CV charges due to the carbon support and alloy in narrow and wide CV scans, respectively, and are assumed to keep constant during the anodic treatment for simplicity; δQ_{re} is the gain of the narrow CV charge due to the reversible oxide, w is a positive coefficient, and $w \delta Q_{re}$ is the gain of wide CV charge due to the change of the reversible oxide. It can be seen that ΔQ_n is proportional to δQ_{re} and may be regarded as an adequate measure for ΔQ_{re} . However, the situation is different for ΔQ_w .

For samples with high-Ru-alloy degrees, there would be a positive δQ_{re} due to the anodic treatment. Because δQ_{irr} is always negative, the presence of term $w \delta Q_{re}$ makes ΔQ_w less negative than it should be for an adequate measure of ΔQ_{irr} . As a result, $(\Delta Q_n - \Delta Q_w)$ would be an underestimate of $(\Delta Q_{re} - \Delta Q_{irr})$, and therefore, k would appear larger. For samples with low alloy degrees, the situation is opposite to that of high-alloy-degree samples, $w \delta Q_{re}$ would be negative and make $(\Delta Q_n - \Delta Q_w)$ an overestimate of $(\Delta Q_{re} - \Delta Q_{irr})$, resulting in a smaller k . These predications are in agreement with Figures 8 and 9; that is, the k in Figure 8 is larger than that in Figure 9.

From these discussions on the findings of this work, it may be concluded that the anodic activation effect is mainly caused

by the changes of Ru oxides in the catalyst. The reason for the anodic activation also reveals an important aspect of the structure–activity relationship for PtRu/C catalysts: the reversible Ru oxide is beneficial and the irreversible Ru oxide harmful. With this point in mind, the apparent conflict between the report on PtRu black catalysts by Rolison and co-workers¹⁹ and that by Briss and co-workers⁵⁰ seems interpretable. Rolison and co-workers first noted the importance of Ru hydrous oxide to the PtRu catalysts for methanol oxidation, but they did not distinguish between the active and harmful oxides.¹⁹ They found that the activity of PtRu black (50:50) for methanol oxidation was depressed by 2 orders of magnitude on reducing in 10% hydrogen at 100 °C for 2 h, and the activity was partially recovered (for 1 order of magnitude) by reoxidation in water-saturated oxygen at 100 °C for 20 h. On the other hand, Briss and co-workers recently reported that the activity of PtRu (50:50) black was improved by reducing in hydrogen at 100 °C for 2–3 h. It should be noted that the condition of reductive treatment used by Briss was stronger than that by Rolison, but the activity was improved rather than severely depressed as Rolison reported. The two apparently opposite reports, however, may be understood on the basis of their CV curves. The CV curves indicated that the actual effects of reduction in hydrogen were different in the two works. In the work of Briss et al, the reduction in hydrogen did not appreciably decrease the CV charge of the reversible oxide, while the character of the irreversible oxide was largely removed from the CV curve (Figure 1 in ref 50). This may explain why the reduced catalyst was more active than the as-received catalyst. In the work of Rolison et al, the reduction in hydrogen caused a large decrease of both oxides with the reversible one decreased most (Figure 2 in ref 19), resulting in a severe decrease in activity. After reoxidation, the total CV charge was partially recovered; however, the CV peak of irreversible oxide seemed larger than the original, and the reversible one was not fully recovered. This may explain why the activity was only partially recovered.

4. Summary

Anodic treatment at 1.3 V versus RHE for 0.5 h in acidic media was found to remarkably improve the activity of PtRu/C catalysts for methanol oxidation. The main reason for the improvement of catalytic activity is the decrease of irreversible Ru (hydrous) oxide, and for high-Ru-alloy-degree catalysts, the production of new reversible Ru (hydrous) oxide also contributes. This finding provides a practical way to improve the catalytic activity of PtRu/C catalysts and the electrodes made from these catalysts for methanol oxidation. Moreover, this finding reveals an important aspect of the structure–activity relationship for PtRu/C catalysts: the reversible Ru (hydrous) oxide is beneficial and the irreversible Ru (hydrous) oxide harmful.

Acknowledgment. This work was supported by the National Key Fundamental R&D Program (TG2000026408), the National Hi-Tech R&D Program (2002AA517030), and the Natural Science Foundation of China (20122101).

References and Notes

- (1) Petry, O. A.; Podlovchenko, B. I.; Frumkin, A. N.; Lal, H. *J. Electroanal. Chem.* **1965**, *10*, 253.
- (2) Andrew, M. R.; Glazebrook, R. W. in *An Introduction to Fuel Cells*; Williams, K. R., Ed.; Elsevier: New York, 1966; p 127.
- (3) Watanabe, M.; Motto, M. *J. Electroanal. Chem.* **1975**, *60*, 275.
- (4) McNicol, B. D.; Short, R. T. *J. Electroanal. Chem.* **1977**, *81*, 249.

- (5) Aricò, A. S.; Srinivasan, S.; Antonucci, V. *Fuel Cells* **2001**, *1* (2), 1.
- (6) Yajima, T.; Wakabayashi, N.; Uchida, H.; Watanabe, M. *Chem. Commun.* **2003**, 828.
- (7) Hogarth, M. P.; Hards, G. A. *Platinum Met. Rev.* **1996**, *40*, 150.
- (8) Franaszczuk, K.; Sobkowski, J. *J. Electroanal. Chem.* **1992**, 327, 235.
- (9) Ley, K. L.; Liu, R. X.; Pu, C.; Fan, Q. B.; Leyarowska, N.; Segre, C.; Smotkin, E. S. *J. Electrochem. Soc.* **1997**, *144*, 1543.
- (10) Frelink, T.; Visscher, W.; Cox, A. P.; Veen, J. V. *Electrochim. Acta* **1995**, *40*, 1537.
- (11) Iwasita, T.; Hoster, H.; John-Anacker, A.; Lin, W. F.; Vielstich, W. *Langmuir* **2000**, *16*, 522.
- (12) Hogarth, M. P.; Ralph, T. R. *Platinum Met. Rev.* **2002**, *46*, 146.
- (13) Aricò, A. S.; Antonucci, P. L.; Modica, E.; Baglio, V.; Kim, H.; Antonucci, V. *Electrochim. Acta* **2002**, *47*, 3723.
- (14) Gasteiger, H. A.; Marković, N.; Ross, P. N., Jr.; Cairns, E. J. *J. Electrochem. Soc.* **1994**, *141*, 1795.
- (15) Gasteiger, H. A.; Marković, N.; Ross, P. N., Jr.; Cairns, E. J. *J. Phys. Chem.* **1993**, *97*, 12020.
- (16) Richarz, F.; Wohlmann, B.; Vogel, U.; Hoffschulz, H.; Wandelt, K. *Surf. Sci.* **1995**, 335, 361.
- (17) Frelink, T.; Visscher, W.; van Veen, J. A. R. *Langmuir* **1996**, *12*, 3702.
- (18) Chu, D.; Gilman, S. *J. Electrochem. Soc.* **1996**, *143*, 1685.
- (19) Long, J. W.; Stroud, R. M.; Swider-Lyons, K. E.; Rolison, D. R. *J. Phys. Chem. B* **2000**, *104*, 9772.
- (20) Rolison, D. R.; Hagans, P. L.; Swider, K. E.; Long, J. W. *Langmuir* **1999**, *15*, 774.
- (21) Koper, M.; Shubina, T.; Santen, R. *J. Phys. Chem. B* **2002**, *106*, 686.
- (22) Watanabe, M.; Uchida, M.; Motoo, S. *J. Electroanal. Chem.* **1987**, *229*, 395.
- (23) Jusys, Z.; Schmidt, T. J.; Dubau, L.; Lasch, K.; Jörissen, L.; Garche, J.; Behm, R. *J. Power Sources* **2002**, *105*, 297.
- (24) Kennedy, B. J.; Hamnett, A. *J. Electroanal. Chem.* **1990**, *283*, 271.
- (25) Aricò, A. S.; Shukla, A. K.; el-Khatib, K. M.; Creti, P.; Antonucci, V. *J. Appl. Electrochem.* **1999**, *29*, 671.
- (26) Aricò, A. S.; Creti, P.; Kim, H.; Mantegna, R.; Giordano, N.; Antonucci, V. *J. Electrochem. Soc.* **1996**, *143*, 3950.
- (27) Goodenough, J. B.; Hamnett, A.; Kennedy, B. J.; Manoharan, R.; Weeks, S. A. *J. Electroanal. Chem.* **1988**, *240*, 133.
- (28) Mahmood, T.; William, J. O.; Miles, R.; McNicol, B. D. *J. Catal.* **1981**, *72*, 218.
- (29) Buckley, A. N.; Kennedy, B. J. *J. Electroanal. Chem.* **1991**, *302*, 261.
- (30) Hamnett, A.; Kennedy, B. J.; Wagner, F. E. *J. Catal.* **1990**, *124*, 30.
- (31) O'Grady, W. E.; Hagans, P. L.; Pandya, K. I.; Maricle, D. L. *Langmuir* **2001**, *17*, 3047.
- (32) Rolison, D. R. *Science* **2003**, *299*, 1698.
- (33) Stroud, R. A.; Long, J. W.; Swider-Lyons, K. E.; Rolison, D. R. *Microsc. Microanal.* **2002**, *8*, 50.
- (34) Aricò, A. S.; Creti, P.; Modica, E.; Monforte, G.; Baglio, V.; Antonucci, V. *Electrochim. Acta* **2000**, *45*, 4319.
- (35) Aricò, A. S.; Shukla, A. K.; K. el-Khatib, M.; Creti, P.; Antonucci, V. *J. Appl. Electrochem.* **1999**, *29*, 671.
- (36) Ren, X. M.; Wilson, M. S.; Gottesfeld, S. *J. Electrochem. Soc.* **1996**, *143*, L12.
- (37) Spinacé, E. V.; Neto, A. O.; Linardi, M. *J. Power Sources* **2004**, *129*, 121.
- (38) Lasch, K.; Hayn, G.; Jörissen, L.; Garche, J.; Besenhardt, O. *J. Power Sources* **2002**, *105*, 305.
- (39) Yang, B.; Lu, Q.; Wang, Y.; Zhuang, L.; Lu, J.; Liu, P.; Wang, J.; Wang, R. *Chem. Mater.* **2003**, *15*, 3552.
- (40) Pozio, A.; De Francesco, M. *J. Power Sources* **2002**, *105*, 13.
- (41) Gong, S.; Lu, J.; Yan, H. *J. Electroanal. Chem.* **1997**, *436*, 291.
- (42) Antolini, E.; Cardellini, F. *J. Alloy Comp.* **2001**, *315*, 118.
- (43) Antolini, E.; Cardellini, F.; Giorgi, L.; Passalacqua, E. *J. Mater. Sci. Lett.* **2000**, *19*, 2099.
- (44) Radmilovic, V.; Gasteiger, H. A.; Ross, P. N., Jr. *J. Catal.* **1995**, *154*, 98.
- (45) Beden, B.; Kadirgan, F.; Lamy, C.; Leger, J. M. *J. Electroanal. Chem.* **1981**, *127*, 75.
- (46) Green, C. L.; Kucernak, A. *J. Phys. Chem. B* **2002**, *106*, 1036.
- (47) Dmowski, W.; Egami, T.; Swider-Lyons, K.; Love, C.; Rolison, D. *J. Phys. Chem. B* **2002**, *106*, 12677.
- (48) Zheng, J. P.; Cygan, P. J.; Jow, T. R. *J. Electrochem. Soc.* **1995**, *142*, 2699.
- (49) Zheng, J. P.; Huang, C. K. *J. New Mater. Electrochem. Syst.* **2002**, *5*, 41.
- (50) Sirk, A. H. C.; Hill, J. M.; Kung, S. K. Y.; Birss, V. I. *J. Phys. Chem. B* **2004**, *108*, 689.